Challenge in realizing de-Sitter space in large scale of Calabi-Yau compactifications

Xin Gao (高 昕)

Sichuan University

Axion 2023

@ Xi'an, 2023.07.25

Outline

Outline

Flux Compactification

- Perturbative superstring provides a quantum gravity theory in 10D.
- From string to the real world: 10D $\rightarrow$ 4D
- What we want: 4D $\mathcal{N} = 1$ Supersymmetry with chiral spectrum

Flux Compactification

- Perturbative superstring provides a quantum gravity theory in 10D.
- From string to the real world: 10D $\rightarrow$ 4D
- What we want: 4D $\mathcal{N} = 1$ Supersymmetry with chiral spectrum
- Best under control: $\mathcal{N} = 1$ Flux Compactification
  - Het string on Calabi-Yau 3-folds (CY_3)
  - Type IIA/B on CY_3 with orientifold (include Type I $\cong$ Type IIB orientifold with $O9$-plane)
  - (Aux 12D) F-theory on CY_4
  - (11D) M-theory on $CY_3 \times S^1/\mathbb{Z}_2$ or on $\mathcal{M}^7$ with G_2 holonomy

Flux Compactification

- Perturbative superstring provides a quantum gravity theory in 10D.
- From string to the real world: 10D $\rightarrow$ 4D
- What we want: 4D $\mathcal{N} = 1$ Supersymmetry with chiral spectrum
- Best under control: $\mathcal{N} = 1$ Flux Compactification
  - Het string on Calabi-Yau 3-folds (CY_3)
  - Type IIA/B on CY_3 with orientifold (include Type I $\cong$ Type IIB orientifold with $O9$-plane)
  - (Aux 12D) F-theory on CY_4
  - (11D) M-theory on $CY_3 \times S^1/\mathbb{Z}_2$ or on $\mathcal{M}^7$ with G_2 holonomy
- Background Flux (in Type II):
  - *Neveu-Schwarz flux:* $H_3 = dB_2, \quad dH_3 = 0.$
  - *Ramond flux:* $F_{p+1} = dC_p, \quad dF_{p+1} = 0.$
  - *Non-geometric flux*
- Considering the flux, the geometry of the CY reacts back mildly by acquiring a non-trivial warp factor as $\mathcal{M}_4 \times X_6$:

$$ds^2 = h(y)^{-1/2} g_{\mu\nu}(x) dx^\mu dx^\nu + h(y)^{1/2} g_{mn}(y) dy^m dy^n$$

where $h(y) \equiv e^{2A(y)}$ is the warp factor, $\mu, \nu = 1, \ldots, 4$, $m, n = 5, \ldots, 10.$

de-Sitter in String Theory I

- At least 3 potential terms with different falloff and appropriate coefficients are needed to get dS. ($\overline{D3}$/T-brane/nilpotent chiralfield uplift potential)

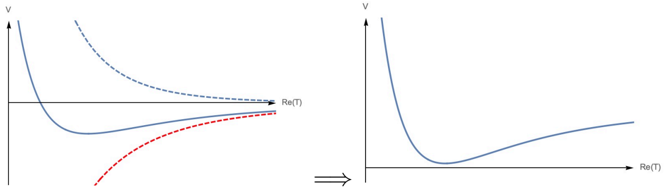

de-Sitter in String Theory I

- At least 3 potential terms with different falloff and appropriate coefficients are needed to get dS. ($\overline{D3}$/T-brane/nilpotent chiralfield uplift potential)

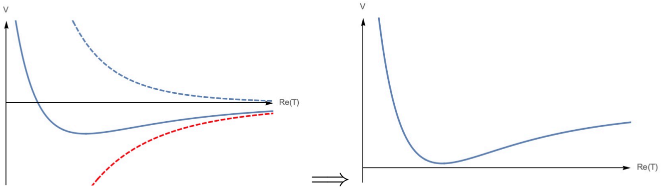

- If all parameters are $\mathcal{O}(1)$, this can never happen in parametric control.
- Swampland conjecture: A potential $V(\phi)$ for scalar fields in a low energy EFT of any consistent QG must satisfy:

$$V'/V \gtrsim \mathcal{O}(1)$$

Ogrui/Palti/Shiu/Vafa

de-Sitter in String Theory I

- At least 3 potential terms with different falloff and appropriate coefficients are needed to get dS. ($\overline{D3}$/T-brane/nilpotent chiralfield uplift potential)

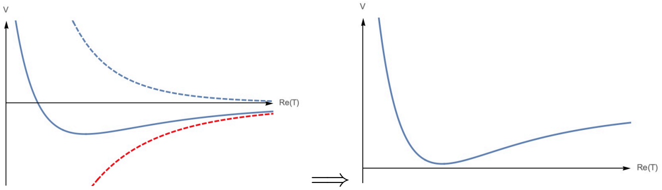

- If all parameters are $\mathcal{O}(1)$, this can never happen in parametric control.
- Swampland conjecture: A potential $V(\phi)$ for scalar fields in a low energy EFT of any consistent QG must satisfy:

$$V'/V \gtrsim \mathcal{O}(1)$$

Oogrui/Palti/Shiu/Vafa

- String Swampland vs. String Landscape

de-Sitter in String Theory II

However, with some tuning of fluxes, de-Sitter space can be realized in Type IIB compactified on orientifold Calabi-Yau threefolds X:

- KKLT and Large Volume Scenario (LVS)
  Kachru/Kallosh/Linde/Trivedi, Valasubramanian/Berglund/Conlon/Quevedo

de-Sitter in String Theory II

However, with some tuning of fluxes, de-Sitter space can be realized in Type IIB compactified on orientifold Calabi-Yau threefolds X:

- KKLT and Large Volume Scenario (LVS)
  Kachru/Kallosh/Linde/Trivedi, Valasubramanian/Berglund/Conlon/Quevedo
- Type IIB is $\mathcal{N}=2$. Break half SUSY to get $\mathcal{N}=1$.
- When consider flux and D-brane, O-plane must be there for tadpole cancelation.

de-Sitter in String Theory II

However, with some tuning of fluxes, de-Sitter space can be realized in Type IIB compactified on orientifold Calabi-Yau threefolds X:

- KKLT and Large Volume Scenario (LVS)
  Kachru/Kallosh/Linde/Trivedi, Valasubramanian/Berglund/Conlon/Quevedo
- Type IIB is $\mathcal{N}=2$. Break half SUSY to get $\mathcal{N}=1$.
- When consider flux and D-brane, O-plane must be there for tadpole cancelation.
- Most of the string phenomenology is building in Type IIB Calabi-Yau orientifold with $O3/O7$-plane.

$$\mathcal{O}=\begin{cases}\Omega_p\,\sigma & \text{with} \quad \sigma^*(J)=J\,, \quad \sigma^*(\Omega_3)=\Omega_3\,, \quad O5/O9 \\ (-)^{F_L}\,\Omega_p\,\sigma & \text{with} \quad \sigma^*(J)=J\,, \quad \sigma^*(\Omega_3)=-\Omega_3\,, \quad O3/O7\end{cases}$$

each σ defines a new CY in the orbifold limit unless it is free action.

de-Sitter in String Theory II

However, with some tuning of fluxes, de-Sitter space can be realized in Type IIB compactified on orientifold Calabi-Yau threefolds X:

- KKLT and Large Volume Scenario (LVS)
  Kachru/Kallosh/Linde/Trivedi, Valasubramanian/Berglund/Conlon/Quevedo
- Type IIB is $\mathcal{N}=2$. Break half SUSY to get $\mathcal{N}=1$.
- When consider flux and D-brane, O-plane must be there for tadpole cancelation.
- Most of the string phenomenology is building in Type IIB Calabi-Yau orientifold with $O3/O7$-plane.

$$\mathcal{O}=\begin{cases}\Omega_p\,\sigma & \text{with} \quad \sigma^*(J)=J\,, \quad \sigma^*(\Omega_3)=\Omega_3\,, \quad O5/O9\\ (-)^{F_L}\,\Omega_p\,\sigma & \text{with} \quad \sigma^*(J)=J\,, \quad \sigma^*(\Omega_3)=-\Omega_3\,, \quad O3/O7\end{cases}$$

each σ defines a new CY in the orbifold limit unless it is free action.

- In orientifold Type IIB, Complex,dilaton moduli decoupled with Kähler moduli.
  - Complex and dilaton moduli can be stabilized by background fluxes at tree level. Gukov/Vafa/Witten
  - Kähler moduli can be stabilized by non-perturbative effects (KKLT, LVS).

KKLT and LVS

KKLT/LVS $\Rightarrow$ meta-stable dS vacua in 3-steps:

- Stabilize complex and dilaton moudli of orientifold CYs by fluxes, leading to a non-SUSY Minkowski minimum($W = W_0 \neq 0$, $V = 0$). Gukov/Vafa/Witten

$$W_{\tau, U} = \int_X G_3 \wedge \Omega, \qquad G_3 = F_3 - \tau H_3$$

- Stabilize Kähler moduli by all possible perturbative and non-perturbative corrections.

$$\begin{aligned} K &= K_{tree} + K_p + K_{np} \\ W &= W_{tree} + W_{np} \end{aligned}$$

leads to corrections of the scalar potential:

$$\delta V = \delta V_{\alpha'} + \delta V_{np}$$

- Uplift to de -Sitter

Can KKLT/LVS be realized in Calabi-Yau compactifications?

- Various corrections in orientifold Type IIB string theory.

Can KKLT/LVS be realized in Calabi-Yau compactifications?

- Various corrections in orientifold Type IIB string theory.
- Parameter constraint in KKLT/LVS by various corrections.

Can KKLT/LVS be realized in Calabi-Yau compactifications?

- Various corrections in orientifold Type IIB string theory.
- Parameter constraint in KKLT/LVS by various corrections.
- Can these constraints be satisfied in large-scale CY compactifications?

Can KKLT/LVS be realized in Calabi-Yau compactifications?

- Various corrections in orientifold Type IIB string theory.
- Parameter constraint in KKLT/LVS by various corrections.
- Can these constraints be satisfied in large-scale CY compactifications?
- Construction of (orientifold) CY manifold and generate CY database

Can KKLT/LVS be realized in Calabi-Yau compactifications?

- Various corrections in orientifold Type IIB string theory.
- Parameter constraint in KKLT/LVS by various corrections.
- Can these constraints be satisfied in large-scale CY compactifications?
- Construction of (orientifold) CY manifold and generate CY database
- Machine learning in searching string vacua

Outline

Corrections in orientifold Type IIB from 10D view

XG/Hebecker/Schreyer/Venken JHEP 09(2022)091

- Warping correction $A(y)$: coming from the back reaction of flux and brane to the geometry (Classical).

Corrections in orientifold Type IIB from 10D view

XG/Hebecker/Schreyer/Venken JHEP 09(2022)091

- Warping correction $A(y)$: coming from the back reaction of flux and brane to the geometry (Classical).
- Generic loop correction: coming from loops of 10d or brane-localized fields propagating in the compact space.
  - non-locality: They can not be associated with local operators in 10d or on a brane (analogous to casimir energy).

Corrections in orientifold Type IIB from 10D view

XG/Hebecker/Schreyer/Venken JHEP 09(2022)091

- Warping correction $A(y)$: coming from the back reaction of flux and brane to the geometry (Classical).
- Generic loop correction: coming from loops of 10d or brane-localized fields propagating in the compact space.
  - non-locality: They can not be associated with local operators in 10d or on a brane (analogous to casimir energy).
- Local α' correction: coming from higher-dimension local operators in bulk, or on the brane system.
  - may receive contributions from the counterterms to renormalize the loops.
  - marginal local operators at α'^4 introduce logarithmic corrections to the Kahler potential.

Loop corrections: BHP conjecture

- String loop corrections are potentially dangerous for LVS, although subleading effects. Cicoli/Conlon/Quevedo
- It only have been concreted calculated in torus cases Berg/Haack/Kors and conjectured in CYs case, the so-called Berg-Haack-Pajer (BHP) conjecture Berg/Haack/Pajer
  - Kaluza-Klein type (exchange KK momentum between branes)
  - Winding type (exchange winding strings between intersecting D7-branes)

$$\delta K^{KK}_{(g_s)} \sim \sum_a \frac{g_s \mathcal{T}_a(t^i)}{\mathcal{V}} \sim \frac{g_s}{\tau}\,, \qquad \delta K^{W}_{(g_s)} \sim \sum_a \frac{1}{\mathcal{I}_a(t^i)\mathcal{V}} \sim \frac{1}{\sqrt{\tau}\mathcal{V}}\,.$$

where $\mathcal{T}_a(t^i)$, $\mathcal{I}_a(t^i)$ linear in 2-cycle.

Loop corrections: BHP conjecture

- String loop corrections are potentially dangerous for LVS, although subleading effects. Cicoli/Conlon/Quevedo
- It only have been concreted calculated in torus cases Berg/Haack/Kors and conjectured in CYs case, the so-called Berg-Haack-Pajer (BHP) conjecture Berg/Haack/Pajer
  - Kaluza-Klein type (exchange KK momentum between branes)
  - Winding type (exchange winding strings between intersecting D7-branes)

$$\delta K^{KK}_{(g_s)} \sim \sum_a \frac{g_s \mathcal{T}_a(t^i)}{\mathcal{V}} \sim \frac{g_s}{\tau}\,, \qquad \delta K^{W}_{(g_s)} \sim \sum_a \frac{1}{\mathcal{I}_a(t^i)\mathcal{V}} \sim \frac{1}{\sqrt{\tau}\mathcal{V}}\,.$$

  where $\mathcal{T}_a(t^i)$, $\mathcal{I}_a(t^i)$ linear in 2-cycle.

- We want to derive statement of BHP-conjecture studying directly loops effects on CYs (using 10d field theory)

Genuine Loop correction

- Consider how loop corrections to kinetic term of volume modulus scale. In one moduli case without flux, compactify Type IIB action on

$$ds^2 = g_{\mu\nu}\, dx^\mu\, dx^\nu + L(x)^2 \tilde{g}_{mn}\, dy^m\, dy^n \qquad \text{where} \qquad \mathcal{V} = L^6$$

$$S = \frac{1}{2\kappa_{10}^2} \int dx^4 \sqrt{-g} L^6 \left[R_4 + 6(6-1) \frac{(\partial L)^2}{L^2} + \cdots \right].$$

Genuine Loop correction

- Consider how loop corrections to kinetic term of volume modulus scale. In one moduli case without flux, compactify Type IIB action on

$$ds^2 = g_{\mu\nu} dx^\mu dx^\nu + L(x)^2 \tilde{g}_{mn} dy^m dy^n \qquad \text{where} \qquad \mathcal{V} = L^6$$

$$S = \frac{1}{2\kappa_{10}^2} \int dx^4 \sqrt{-g} L^6 \left[R_4 + 6(6-1)\frac{(\partial L)^2}{L^2} + \cdots \right].$$

- Loop corrections induced by integrating out KK modes of mass. From both dimensional analyze and Feynman-Diagram calculations:

$$\delta S_{1-\text{loop}} = \int dx^4 \sqrt{-g} \left(\frac{b_0}{L^2} R_4 + \frac{b_1}{L^4} (\partial L)^2 \right)$$

Genuine Loop correction

- Consider how loop corrections to kinetic term of volume modulus scale. In one moduli case without flux, compactify Type IIB action on

$$ds^2 = g_{\mu\nu} dx^\mu dx^\nu + L(x)^2 \tilde{g}_{mn} dy^m dy^n \qquad \text{where} \qquad \mathcal{V} = L^6$$

$$S = \frac{1}{2\kappa_{10}^2} \int dx^4 \sqrt{-g} L^6 \left[R_4 + 6(6-1) \frac{(\partial L)^2}{L^2} + \cdots \right].$$

- Loop corrections induced by integrating out KK modes of mass. From both dimensional analyze and Feynman-Diagram calculations:

$$\delta S_{1-\text{loop}} = \int dx^4 \sqrt{-g} \left(\frac{b_0}{L^2} R_4 + \frac{b_1}{L^4} (\partial L)^2 \right)$$

- Consider 4-cycle as $\tau \sim M_{10}^4 L^4$, the Kähler potential will reads:

$$(S + \delta S)_{\text{EF}} = \frac{M_4^2}{2} \int d^4 x \sqrt{-g} \left[R_4 + \left(-\frac{3}{2} \frac{(\partial\tau)^2}{\tau^2} + \frac{114 b_0 + b_1}{32\pi} \frac{(\partial\tau)^2}{\tau^4} \right) \right]$$

$$K + \delta K_{1-\text{loop}} \sim 1/\tau^2 + 1/\tau^4 \quad \Rightarrow \quad \delta K_{1-\text{loop}} \sim 1/\tau^2 \sim \frac{1}{\sqrt{\tau}\mathcal{V}}$$

scales like BHP winding correction. Unlike BHP, it is not tied to intersecting branes (non-local) and the linearity on 2-cycle volume does not appear in multi-molduli case.

Local α' corrections

- Coming higher-dimension local operators in 10d.
  In Einstein frame, the purely gravitational curvature part of type IIB:

$$S_{\text{EF}} \sim \int dx^{10}\sqrt{-g}\left[M_{10}^8 R_{10} + \frac{M_{10}^2}{g_s^{3/2}} R_{10}^4 + M_{10}^2 g_s^{1/2} R_{10}^4 + \mathcal{O}\left(M_{10}^{-2} g_s^{-5/2} R_{10}^6\right)\right]$$

Antoniadis/Ferrara/Minasian/Narain

Local α' corrections

- Coming higher-dimension local operators in 10d.
In Einstein frame, the purely gravitational curvature part of type IIB:

$$S_{\text{EF}} \sim \int dx^{10}\sqrt{-g}\left[M_{10}^8 R_{10} + \frac{M_{10}^2}{g_s^{3/2}} R_{10}^4 + M_{10}^2 g_s^{1/2} R_{10}^4 + \mathcal{O}\left(M_{10}^{-2} g_s^{-5/2} R_{10}^6\right)\right]$$

Antoniadis/Ferrara/Minasian/Narain

- Contributions from high momentum region of integral. Part of the term $M_{10}^2 g_s^{1/2} R_{10}^4$ can be identified as a counterterm of our EFT analysis.
- Correction to 4D Kahler potential comes from higher dimensional operators compact to 4d. For example R_{10}^4 terms:

$$\left(\frac{M_{10}^2}{g_s^{3/2}} + M_{10}^2 g_s^{1/2}\right) R_{\text{external}} \int dx^6 R_{\text{internal}}^3 \sim \left(\frac{M_{10}^2}{g_s^{3/2}} + M_{10}^2 g_s^{1/2}\right) R_{\text{external}}$$

reproduces the well known string tree-level BBHL correction Becker/Becker/Haack/Louis and its 1-loop counterpart.

Corrections on D7/O7

Correction type	Induced by	Correction to Kahler potential	Correction to scalar potential
Genuine loops	-	f_{-2}	$\|W_0\|^2 g_s \times h_{-5}$
BBHL+1-loop	$\frac{M_{10}^2}{g_s^{3/2}}(1+g_s^2)R_{10}^4$	$(g_s^{-1/2}+g_s^{3/2}) \times f_{-3/2}$	$\|W_0\|^2(g_s^{-3/2}+g_s^{1/2}) \times h_{-9/2}$
Non-intersecting D7/O7 (partly)	$M_{10}^4(1+g_s)R_8^2$	$(0+g_s)\times f_{-1}$	$\|W_0\|^2 g_s^3 \times h_{-5}$
Log-Correction on D7/O7	R_8^4	$\ln(M_{10}g_s^{1/4}L) \times f_{-2}$	$\|W_0\|^2 g_s \ln(M_{10}g_s^{1/4}L) \times h_{-5}$
Intersecting D7/O7	$M_{10}^4(1+g_s)R_6$	$(0+g_s)\times f_{-1}$	$\|W_0\|^2 g_s^3 \times h_{-5}$
Log-Correction on intersecting D7/O7	R_6^3	$\ln(M_{10}g_s^{1/4}L) \times f_{-2}$	$\|W_0\|^2 g_s \ln(M_{10}g_s^{1/4}L) \times h_{-5}$

- $f_{-\lambda}, h_{-\lambda}$ are homogeneous of degree $-\lambda$ in 4-cycles τ.
- g_s/f_{-1}: scaling like BHP KK correction (indeed in Brane system).
- log enhanced loop correction from marginal operator.
- Genuine loop corrections scale like BHP winding correction. However, in multi Kähler moduli case, scaling persists but linearity is not found in fiberd geometry like K3 fibered on $\mathbb{P}^1$.

Outline

Tadpole Cancelation

The geometry with strongly warped throat in Type IIB is locally described by Klebanov-Strassler (KS) solution.

Klebanov/Strassler, Giddings/Karchru/Polchinski

The fluxes number is given by fluxes warpping on two 3-cycles at the conifold :

$$M = \int_A H_3, \quad K = \int_B F_3,$$

The throat carries $N = K \cdot M$ units of D3-brane charge contribute to tadpole.

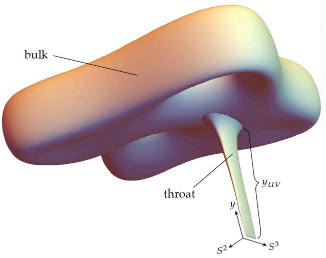

from Ralph's paper

Tadpole Cancelation

The geometry with strongly warped throat in Type IIB is locally described by Klebanov-Strassler (KS) solution.

Klebanov/Strassler, Giddings/Karchru/Polchinski

The fluxes number is given by fluxes warpping on two 3-cycles at the conifold :

$$M = \int_A H_3, \quad K = \int_B F_3,$$

The throat carries $N = K \cdot M$ units of D3-brane charge contribute to tadpole.

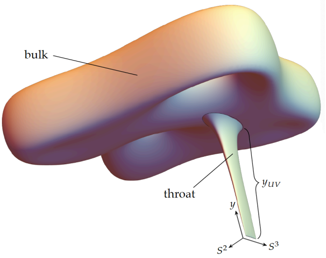

from Ralph's paper

- With $N_{\rm flux} = 2N = 2KM$, the $D3$ tadpole is generally given by

$$N_{D3} + \frac{N_{\sf flux}}{2} + N_{\sf gauge} = \frac{N_{O3}}{4} + \frac{\chi(D_{O7})}{12} + \sum_a N_a \frac{\chi(D_a) + \chi(D'_a)}{48} \equiv -Q_3 ,$$

Tadpole Cancelation

The geometry with strongly warped throat in Type IIB is locally described by Klebanov-Strassler (KS) solution.

Klebanov/Strassler, Giddings/Karchru/Polchinski

The fluxes number is given by fluxes warpping on two 3-cycles at the conifold :

$$M = \int_A H_3, \quad K = \int_B F_3,$$

The throat carries $N = K \cdot M$ units of D3-brane charge contribute to tadpole.

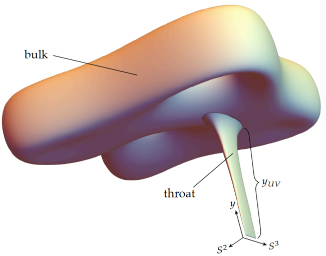

from Ralph's paper

- With $N_{\rm flux} = 2N = 2KM$, the $D3$ tadpole is generally given by

$$N_{D3} + \frac{N_{\rm flux}}{2} + N_{\rm gauge} = \frac{N_{O3}}{4} + \frac{\chi(D_{O7})}{12} + \sum_a N_a \frac{\chi(D_a) + \chi(D'_a)}{48} \equiv -Q_3 \,,$$

- Locally, $N_{D3} + N + N_{\rm gauge} = \frac{N_{O3}}{4} + \frac{\chi(D_{O7})}{4} \equiv -Q_3$

Tadpole Cancelation

The geometry with strongly warped throat in Type IIB is locally described by Klebanov-Strassler (KS) solution.

Klebanov/Strassler, Giddings/Karchru/Polchinski

The fluxes number is given by fluxes warpping on two 3-cycles at the conifold :

$$M = \int_A H_3, \quad K = \int_B F_3,$$

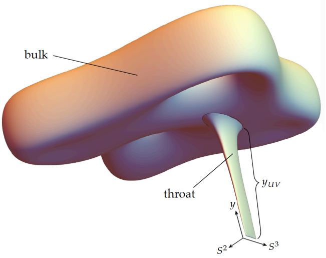

from Ralph's paper

The throat carries $N = K \cdot M$ units of D3-brane charge contribute to tadpole.

- With $N_{\text{flux}} = 2N = 2KM$, the $D3$ tadpole is generally given by

$$N_{D3} + \frac{N_{\text{flux}}}{2} + N_{\text{gauge}} = \frac{N_{O3}}{4} + \frac{\chi(D_{O7})}{12} + \sum_a N_a \frac{\chi(D_a) + \chi(D_a')}{48} \equiv -Q_3 \,,$$

- Locally, $N_{D3} + N + N_{\text{gauge}} = \frac{N_{O3}}{4} + \frac{\chi(D_{O7})}{4} \equiv -Q_3$
- Tadpole condition: We must at least have sufficient negative tadpole Q_3 to cancel the flux in the throat

$$-Q_3 > N$$

.

KKLT Scenario

Kachru/Kallosh/Linde/Trivedi

Only Non-perturbative correction to superpotential
$\Rightarrow$ Fine-tune tree level superpotential W_0

- Stabilize Kähler moduli:

  Non-perturbative effects (E3-instanton (E3 on 4-cycle Σ)/gaugino condensation (D7)) stabilize the Kähler moduli T, leading to an SUSY AdS minimum V_{AdS}.

$$K = -3\ln(T+\overline{T}), \quad W = W_0 + e^{-T}$$

$$V = e^K (K^{T\overline{T}} |\partial_T W + W \partial_T K|^2 - 3|W|^2)$$

$$V_{AdS} \sim -e^{-\mathrm{Re}(T)}$$

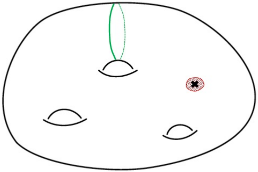

- Uplift to dS:

  Uplift to dS by palcing $\overline{D3}$ in the throat tip, contribute $V_{\text{uplift}} \sim e^{-K/g_s M}$.

  Meta-stable if uplift energy is not too large:

$$V_{\text{uplift}} \sim |V_{AdS}| \;\Rightarrow\; \mathrm{Re}(T) \sim \frac{N}{g_s M^2}$$

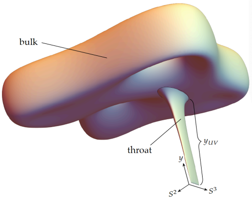

Singular Bulk Problem XG/Junghans/Hebechker Fortsch.Phys.68(2020)2000089

- Kähler moduli $\mathrm{Re}(T)$ in $W_{np} \sim e^{-T}$ is precisely the $E3$-brane action:

$$\mathrm{Re}(T) \sim N/g_s M^2 \sim S_{E3} = \frac{1}{g_s} \int_{\Sigma} \sqrt{g}\, h(y)$$

Singular Bulk Problem XG/Junghans/Hebechker Fortsch.Phys.68(2020)2000089

- Kähler moduli $\mathrm{Re}(T)$ in $W_{np} \sim e^{-T}$ is precisely the $E3$-brane action:

$$\mathrm{Re}(T) \sim N/g_s M^2 \sim S_{E3} = \frac{1}{g_s}\int_\Sigma \sqrt{g}\, h(y)$$

- Then we constrain the warp factor average over the 4-cycle Σ:

$$\langle h(y)\rangle_\Sigma \equiv \frac{\int_\Sigma \sqrt{g}\, h(y)}{\int_\Sigma \sqrt{g}} \sim \frac{N}{M^2 \mathcal{V}_\Sigma} \sim \frac{N}{M^2}$$

Singular Bulk Problem XG/Junghans/Hebechker Fortsch.Phys.68(2020)2000089

- Kähler moduli $\mathrm{Re}(T)$ in $W_{np} \sim e^{-T}$ is precisely the $E3$-brane action:

$$\mathrm{Re}(T) \sim N/g_s M^2 \sim S_{E3} = \frac{1}{g_s}\int_\Sigma \sqrt{g}\, h(y)$$

- Then we constrain the warp factor average over the 4-cycle Σ:

$$\langle h(y)\rangle_\Sigma \equiv \frac{\int_\Sigma \sqrt{g}\, h(y)}{\int_\Sigma \sqrt{g}} \sim \frac{N}{M^2 \mathcal{V}_\Sigma} \sim \frac{N}{M^2}$$

implies in the neihborhood of Σ, there is: $h \lesssim \frac{N}{M^2}$

Singular Bulk Problem XG/Junghans/Hebechker Fortsch.Phys.68(2020)2000089

- Kähler moduli $\mathrm{Re}(T)$ in $W_{np} \sim e^{-T}$ is precisely the $E3$-brane action:

$$\mathrm{Re}(T) \sim N/g_s M^2 \sim S_{E3} = \frac{1}{g_s}\int_\Sigma \sqrt{g}\, h(y)$$

- Then we constrain the warp factor average over the 4-cycle Σ:

$$\langle h(y)\rangle_\Sigma \equiv \frac{\int_\Sigma \sqrt{g}\, h(y)}{\int_\Sigma \sqrt{g}} \sim \frac{N}{M^2 \mathcal{V}_\Sigma} \sim \frac{N}{M^2}$$

  implies in the neihborhood of Σ, there is: $h \lesssim \frac{N}{M^2}$

- h represent a form of 'electrostatic potential' for the D3 charge density ρ_{D3} on the CY:

$$-\nabla^2\ h = g_s \rho_{D3}$$

  implies the variation of the h due to N unit $D3$ charge at the KS-tip: $|\partial h| \equiv \sqrt{g^{mn}(\partial_m h)(\partial_n h)} \sim g_s N$

Singular Bulk Problem XG/Junghans/Hebechker Fortsch.Phys.68(2020)2000089

- Kähler moduli $\mathrm{Re}(T)$ in $W_{np} \sim e^{-T}$ is precisely the $E3$-brane action:

$$\mathrm{Re}(T) \sim N/g_s M^2 \sim S_{E3} = \frac{1}{g_s}\int_\Sigma \sqrt{g}\, h(y)$$

- Then we constrain the warp factor average over the 4-cycle Σ:

$$\langle h(y)\rangle_\Sigma \equiv \frac{\int_\Sigma \sqrt{g}\, h(y)}{\int_\Sigma \sqrt{g}} \sim \frac{N}{M^2 \mathcal{V}_\Sigma} \sim \frac{N}{M^2}$$

  implies in the neihborhood of Σ, there is: $h \lesssim \frac{N}{M^2}$

- h represent a form of 'electrostatic potential' for the D3 charge density ρ_{D3} on the CY:

$$-\nabla^2\ h = g_s \rho_{D3}$$

  implies the variation of the h due to N unit $D3$ charge at the KS-tip: $|\partial h| \equiv \sqrt{g^{mn}(\partial_m h)(\partial_n h)} \sim g_s N$

$$\frac{|\partial h|}{h} \gtrsim \frac{g_s N}{N/M^2} \sim g_s M^2 \gtrsim M \gg 1.$$

  - $g_s M \gtrsim 1$ for small curvature at KS tip (SUGRA control)
    Klebanov/Strassler, Kachru/Pearson/Verlinde(KPV), Klebanov/Herzog/Ouyang
  - $g_s M^2 \gtrsim 12$ for metastability of the $\overline{D3}$ (polarization of $\overline{D3}$ into NS5)
    KPV, Bena/Dudas/Grana/Lust, Blumenhagen/Klawer/Schlechter

How large is the singular region in CY?

- Variation of h much larger than its average $\frac{|\partial h|}{h} \gg 1$. This leads $h < 0$ on $\mathcal{O}(1)$ fraction of $E3$ volume, making much of the $E3$ singular.
- $-\nabla^2\ h = g_s \rho_{D3}$ implies that at least one eigenvalue of $\nabla_m \partial_n h$ is negative.

How large is the singular region in CY?

- Variation of h much larger than its average $\frac{|\partial h|}{h} \gg 1$. This leads $h < 0$ on $\mathcal{O}(1)$ fraction of $E3$ volume, making much of the $E3$ singular.
- $-\nabla^2 \, h = g_s \rho_{D3}$ implies that at least one eigenvalue of $\nabla_m \partial_n h$ is negative.
- The singularity will spread over an $\mathcal{O}(1)$ distance into the transverse space, extending over a large part of the Calabi-Yau.

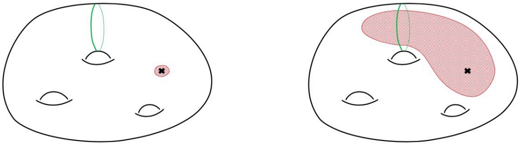

How large is the singular region in CY?

- Variation of h much larger than its average $\frac{|\partial h|}{h} \gg 1$. This leads $h < 0$ on $\mathcal{O}(1)$ fraction of $E3$ volume, making much of the $E3$ singular.
- $-\nabla^2 \ h = g_s \rho_{D3}$ implies that at least one eigenvalue of $\nabla_m \partial_n h$ is negative.
- The singularity will spread over an $\mathcal{O}(1)$ distance into the transverse space, extending over a large part of the Calabi-Yau.

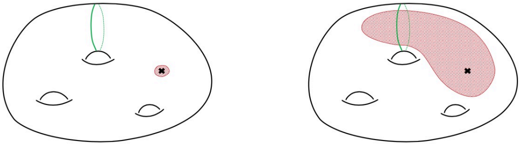

- Alternative view of the problem (curvature scalar):

$$R_6 = h^{-5/2} |\partial h|^2 - 3/2 h^{-3/2} \nabla^2 h \quad \Rightarrow \quad R_6 \gtrsim g_s^2 M^5 / \sqrt{N}$$

Imposing $g_s M \gtrsim 1$, $M \gtrsim 12$ and $R_6 \lesssim 1$ implies $N \gtrsim 3 \cdot 10^6$, exceeds the largest know tadpole of 7.5×10^4 in string compactification. Taylor/Wang

- Warping correction + meta-stable of de-Sitter in KKLT
$\Rightarrow$ Singular Bulk Problem

LVS

Balasubramanian/Berglund/Conlon/Quevedo

Non-perturbative contribution to superpotentail
Perturbative α'^3 correction to Kähler potential $(\tau = \mathrm{Re}(T))$

$$W = W_0 + A_s e^{-a_s T_s}, \quad K = -2\ln\left(\mathcal{V} + \frac{\xi}{2g_s^{3/2}}\right) = -2\ln\left(\tau_b^{3/2} - \kappa_s \tau_s^{3/2} - \frac{\chi(X)\,\zeta(3)}{4(2\pi)^3 g_s^{3/2}}\right)$$

LVS

Balasubramanian/Berglund/Conlon/Quevedo

Non-perturbative contribution to superpotentail
Perturbative α'^3 correction to Kähler potential ($\tau = \mathrm{Re}(T)$)

$$W = W_0 + A_s e^{-a_s T_s}, \quad K = -2\ln\left(\mathcal{V} + \frac{\xi}{2g_s^{3/2}}\right) = -2\ln\left(\tau_b^{3/2} - \kappa_s \tau_s^{3/2} - \frac{\chi(X)\,\zeta(3)}{4(2\pi)^3 g_s^{3/2}}\right)$$

This yields the pure LVS scalar potential

$$V \sim \frac{g_s\sqrt{\tau}_s e^{-2a_s\tau_s}}{\mathcal{V}} - \frac{g_s\tau_s W_0 e^{-a_s\tau_s}}{\mathcal{V}^2} + \frac{\xi W_0^2}{\sqrt{g_s}\mathcal{V}^3}$$

which is minimized by

$$\mathcal{V} = \frac{3\kappa_s |W_0|\sqrt{\tau_s}}{4a_s|A_s|} e^{a_s\tau_s} , \qquad \tau_s = \frac{\xi^{2/3}}{(2\kappa_s)^{2/3} g_s} + \mathcal{O}(1) ,$$

leading to an AdS vacuum at exponentially large volume

$$V_{\mathsf{AdS}} = -\frac{3\kappa_s g_s\sqrt{\tau_s}|W_0|^2}{8a_s\mathcal{V}^3} .$$

LVS

Balasubramanian/Berglund/Conlon/Quevedo

Non-perturbative contribution to superpotentail
Perturbative α'^3 correction to Kähler potential $(\tau = \mathrm{Re}(T))$

$$W = W_0 + A_s e^{-a_s T_s}, \quad K = -2\ln\left(\mathcal{V} + \frac{\xi}{2 g_s^{3/2}}\right) = -2\ln\left(\tau_b^{3/2} - \kappa_s \tau_s^{3/2} - \frac{\chi(X)\,\zeta(3)}{4(2\pi)^3 g_s^{3/2}}\right)$$

This yields the pure LVS scalar potential

$$V \sim \frac{g_s \sqrt{\tau}_s e^{-2a_s\tau_s}}{\mathcal{V}} - \frac{g_s \tau_s W_0 e^{-a_s\tau_s}}{\mathcal{V}^2} + \frac{\xi W_0^2}{\sqrt{g_s}\mathcal{V}^3}$$

which is minimized by

$$\mathcal{V} = \frac{3\kappa_s |W_0| \sqrt{\tau_s}}{4 a_s |A_s|} e^{a_s \tau_s} \ , \qquad \tau_s = \frac{\xi^{2/3}}{(2\kappa_s)^{2/3} g_s} + \mathcal{O}(1)\,,$$

leading to an AdS vacuum at exponentially large volume

$$V_{\mathrm{AdS}} = -\frac{3\kappa_s g_s \sqrt{\tau_s}|W_0|^2}{8 a_s \mathcal{V}^3}\,.$$

LVS expansion balance the perturbative and non-perturbative correction

$$\delta V_{\alpha'} \sim \delta V_{np} \sim \mathcal{O}\left(\frac{1}{\mathcal{V}^3}\right)$$

Control problem also for LVS?

Are there warping corrections associated to the realization of de-Sitter that are deadly for LVS?

Control problem also for LVS?

Are there warping corrections associated to the realization of de-Sitter that are deadly for LVS?

- In principle, LVS is well protected from various correction because the CYs volume is exponentially large.

Control problem also for LVS?

Are there warping corrections associated to the realization of de-Sitter that are deadly for LVS?

- In principle, LVS is well protected from various correction because the CYs volume is exponentially large.
- However, the problem does not disappear since at large volume the AdS minimum of LVS becomes shallow, requiring a small uplift and hence a strongly warped throat. Junghans

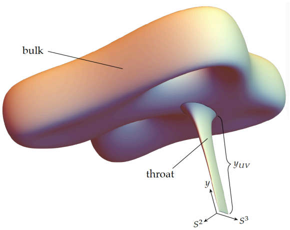

Control problem also for LVS?

Are there warping corrections associated to the realization of de-Sitter that are deadly for LVS?

- In principle, LVS is well protected from various correction because the CYs volume is exponentially large.
- However, the problem does not disappear since at large volume the AdS minimum of LVS becomes shallow, requiring a small uplift and hence a strongly warped throat. Junghans

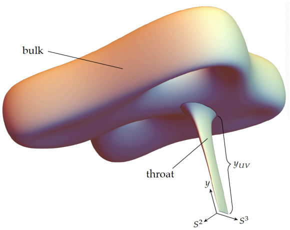

- Warping correction + meta-stable of de-Sitter in LVS
  $\Rightarrow$ Parametric Tadpole Constraint (PTC)

  XG/Hebecker/Schreyer/Venken JHEP 07(2022)056

Warping corrections of LVS

- We derive the most precise formula for warping of anti D3 brane uplift term at tip:

$$V_{\text{up}} = \frac{\left(3^2\,\pi^3\,2^{22/3}\right)^{1/5}}{a_0}\,\frac{e^{-\frac{8\pi N}{3 g_s M^2}}}{g_s M^2 \mathcal{V}^{4/3}}$$

Warping corrections of LVS

- We derive the most precise formula for warping of anti D3 brane uplift term at tip:

$$V_{\rm up} = \frac{\left(3^2\,\pi^3\,2^{22/3}\right)^{1/5}}{a_0}\,\frac{e^{-\frac{8\pi N}{3 g_s M^2}}}{g_s M^2 \mathcal{V}^{4/3}}$$

- meta-stable de-Sitter vacuum means again $V_{\rm up} \approx |V_{AdS}|$ leads to a constrain on the CY volume $\mathcal{V}$ and gives a relation between the parameters of warped throat and bulk CYs.
- Warping correction to Euler number $\chi(X)$:

$$\frac{1}{g_s^{3/2}}\int_{\mathcal{M}_{10}} e^{2A(y)}\, R\wedge R\wedge R\wedge R\wedge e\wedge e \approx \frac{1}{g_s^{3/2}}\int d^4x R_4\left(\chi(X) + \frac{\chi(X)N}{\mathcal{V}^{2/3}}\right)$$

leads to the warping correction to the scalar potential

$$\delta\, V_{warp} = \frac{15\,\xi\, N\,|\,W_0|^2}{8\sqrt{g_s}\,\mathcal{V}^{11/3}}\,\mathcal{O}(1)$$

Warping corrections of LVS

- We derive the most precise formula for warping of anti D3 brane uplift term at tip:

$$V_{\rm up} = \frac{\left(3^2\,\pi^3\,2^{22/3}\right)^{1/5}}{a_0}\,\frac{e^{-\frac{8\pi N}{3 g_s M^2}}}{g_s M^2 \mathcal{V}^{4/3}}$$

- meta-stable de-Sitter vacuum means again $V_{\rm up} \approx |V_{AdS}|$ leads to a constrain on the CY volume $\mathcal{V}$ and gives a relation between the parameters of warped throat and bulk CYs.
- Warping correction to Euler number $\chi(X)$:

$$\frac{1}{g_s^{3/2}}\int_{\mathcal{M}_{10}} e^{2A(y)}\,R\wedge R\wedge R\wedge R\wedge e\wedge e \approx \frac{1}{g_s^{3/2}}\int d^4x R_4\left(\chi(X) + \frac{\chi(X)N}{\mathcal{V}^{2/3}}\right)$$

  leads to the warping correction to the scalar potential

$$\delta\,V_{warp} = \frac{15\,\xi\,N|\,W_0|^2}{8\sqrt{g_s}\,\mathcal{V}^{11/3}}\,\mathcal{O}(1)$$

- A measure for parametric control is given by comparing the size of $\delta\,V_{warp}$ and its value at the minimum V_{AdS}:

$$c_N \equiv \frac{V_{AdS}}{\delta\,V_{warp}}, \qquad \mathcal{V}^{2/3} = c_N\frac{10\,a_s\,\xi^{2/3}}{(2\kappa_s)^{2/3} g_s}N$$

  $\Rightarrow c_N \gg 1$ for parameter control.

Constraints from W_0

- Higher F-terms corrections to the scalar potential (eight derivative terms)
  Ciupke/Louis/Westphal/Junghans

$$\delta V_F \sim \frac{W_0^4 g_s^{1/2}}{\mathcal{V}^{11/3}}$$

  and we introduce another ratio c_{W_0} such that:

$$c_{W_0} \equiv \frac{V_{AdS}}{\delta V_F}, \qquad \frac{1}{W_0^2} = c_{W_0} \frac{16 a_s}{3(2\kappa_s)^{2/3}\xi^{1/3}} \frac{1}{\mathcal{V}^{2/3}}$$

  $\Rightarrow c_{W_0} \gg 1$ for parameter control.

Constraints from W_0

- Higher F-terms corrections to the scalar potential (eight derivative terms) Ciupke/Louis/Westphal/Junghans

$$\delta V_F \sim \frac{W_0^4 g_s^{1/2}}{\mathcal{V}^{11/3}}$$

and we introduce another ratio c_{W_0} such that:

$$c_{W_0} \equiv \frac{V_{AdS}}{\delta V_F}, \qquad \frac{1}{W_0^2} = c_{W_0} \frac{16 a_s}{3(2\kappa_s)^{2/3}\xi^{1/3}} \frac{1}{\mathcal{V}^{2/3}}$$

$\Rightarrow c_{W_0} \gg 1$ for parameter control.

- In addition, there is another bound on the tadpole related to W_0: Denef/Douglas

$$-Q_3 \geq 2\pi g_s W_0^2$$

- Replace $W_0, \mathcal{V}$ in terms of c_{W_0}, c_N and consider the standard Tadpole condition in Type IIB, we have:

$$-Q_3 \geq \frac{c_N}{c_{W_0}} \frac{15\pi\xi}{4} N \equiv c_Q N, \quad -Q_3 > N$$

This result allows for a more compact formulation if we merely restrict c_N and c_{W_0} such that some minimal quality of control is ensured.

Parametric Tadpole Constraint (PTC)

XG/Hebecker/Schreyer/Venken JHEP 07(2022)056

- Replace W_0 and $\mathcal{V}$ in terms of c_{W_0} and c_N, from $V_{up} = |V_{AdS}|$, we will get an equation for N which is of the form $we^w = x$. Then one can give analytic expression of N.
- Combining this set of constraints, one can obtain a constraint on the flux $N = K \cdot M$ required in the warped throat

The LVS parametric tadpole constraint:
The D3 tadpole contribution Q_3 of O3/O7-planes and D7-branes must fulfill

$$-Q_3 > N = N_* \left(\frac{1}{3} \ln N_* + \frac{5}{3} \ln c_N + \ln a_s - \frac{2}{3} \ln \kappa_s + 8.2 + \mathcal{O}(\ln(\ln)) \right),$$

where we defined $\quad N_* = 9 g_s M^2 / (16\pi)$.

Parametric Tadpole Constraint (PTC)

XG/Hebecker/Schreyer/Venken JHEP 07(2022)056

- Replace W_0 and $\mathcal{V}$ in terms of c_{W_0} and c_N, from $V_{up} = |V_{AdS}|$, we will get an equation for N which is of the form $we^w = x$. Then one can give analytic expression of N.
- Combining this set of constraints, one can obtain a constraint on the flux $N = K \cdot M$ required in the warped throat

The LVS parametric tadpole constraint:
The D3 tadpole contribution Q_3 of O3/O7-planes and D7-branes must fulfill

$$-Q_3 > N = N_* \left(\frac{1}{3} \ln N_* + \frac{5}{3} \ln c_N + \ln a_s - \frac{2}{3} \ln \kappa_s + 8.2 + \mathcal{O}(\ln(\ln)) \right),$$

where we defined $N_* = 9 g_s M^2 / (16\pi)$.

- Two parameters c_N and $g_s M^2$
  - $g_s M^2 > 12$ from KPV solution Kachru/Pearson/Verlinde
  - $g_s M^2 > 46$ for stability warped throat Bena/Dudas/Grana/Lust

Lower bound on the tadpole from PTC

The LVS parametric tadpole constraint:
The D3 tadpole contribution Q_3 of O3/O7-planes and D7-branes must fulfill

$$-Q_3 > N = N_* \left(\frac{1}{3} \ln N_* + \frac{5}{3} \ln c_N + \ln a_s - \frac{2}{3} \ln \kappa_s + 8.2 + \mathcal{O}(\ln(\ln)) \right),$$

where we defined $\quad N_* = 9 g_s M^2/(16\pi)$.

- Our PTC provide a lower bound on the required tabpole:
  - $\kappa_s = 1,\ g_s M^2 = 46,\ a_s = \pi/3, c_N = 5 \quad \Rightarrow \quad N = 133$
  - $\kappa_s = 1,\ g_s M^2 = 46,\ a_s = \pi/3, c_N = 100 \quad \Rightarrow \quad N = 180$
  - $\kappa_s = 1,\ g_s M^2 = 90,\ a_s = 2\pi,\ c_N = 5 \quad \Rightarrow \quad N = 298$
  - $\kappa_s = 1,\ g_s M^2 = 90,\ a_s = 2\pi,\ c_N = 100 \quad \Rightarrow \quad N = 388$

Lower bound on the tadpole from PTC

The LVS parametric tadpole constraint:
The D3 tadpole contribution Q_3 of O3/O7-planes and D7-branes must fulfill

$$-Q_3 > N = N_* \left(\frac{1}{3} \ln N_* + \frac{5}{3} \ln c_N + \ln a_s - \frac{2}{3} \ln \kappa_s + 8.2 + \mathcal{O}(\ln(\ln)) \right),$$

where we defined $N_* = 9 g_s M^2/(16\pi)$.

- Our PTC provide a lower bound on the required tabpole:
  - $\kappa_s = 1,\ g_s M^2 = 46,\ a_s = \pi/3, c_N = 5 \quad \Rightarrow \quad N = 133$
  - $\kappa_s = 1,\ g_s M^2 = 46,\ a_s = \pi/3, c_N = 100 \quad \Rightarrow \quad N = 180$
  - $\kappa_s = 1,\ g_s M^2 = 90,\ a_s = 2\pi,\ c_N = 5 \quad \Rightarrow \quad N = 298$
  - $\kappa_s = 1,\ g_s M^2 = 90,\ a_s = 2\pi,\ c_N = 100 \quad \Rightarrow \quad N = 388$
- On the other hand, there is a so-called Tadpole conjecture Bena/Blaback/Grana/Lust, if it is correct, indicates an upper bound, that the tadpole should not be too large in order to stabilize the complex structure moduli of the orientifold CYs.

Lower bound on the tadpole from PTC

The LVS parametric tadpole constraint:
The D3 tadpole contribution Q_3 of O3/O7-planes and D7-branes must fulfill

$$-Q_3 > N = N_* \left(\frac{1}{3} \ln N_* + \frac{5}{3} \ln c_N + \ln a_s - \frac{2}{3} \ln \kappa_s + 8.2 + \mathcal{O}(\ln(\ln)) \right),$$

where we defined $\quad N_* = 9 g_s M^2 / (16\pi)$.

- Our PTC provide a lower bound on the required tabpole:
  - $\kappa_s = 1,\ g_s M^2 = 46,\ a_s = \pi/3, c_N = 5 \quad \Rightarrow \quad N = 133$
  - $\kappa_s = 1,\ g_s M^2 = 46,\ a_s = \pi/3, c_N = 100 \quad \Rightarrow \quad N = 180$
  - $\kappa_s = 1,\ g_s M^2 = 90,\ a_s = 2\pi,\ c_N = 5 \quad \Rightarrow \quad N = 298$
  - $\kappa_s = 1,\ g_s M^2 = 90,\ a_s = 2\pi,\ c_N = 100 \quad \Rightarrow \quad N = 388$
- On the other hand, there is a so-called Tadpole conjecture Bena/Blaback/Grana/Lust, if it is correct, indicates an upper bound, that the tadpole should not be too large in order to stabilize the complex structure moduli of the orientifold CYs.
- Do we have a model satisfy the PTC?

Orientifold Calabi-Yau threefold landscape

- toric CY3 hypersurface ($\# <? \mathcal{O}(10^{920})$) Borisov/Batyrev/Cox/Kreuzer/Skarke/Demirtas/Long/McAllister ......

Orientifold Calabi-Yau threefold landscape

- toric CY3 hypersurface ($\# <? \mathcal{O}(10^{920})$) Borisov/Batyrev/Cox/Kreuzer/Skarke/ Demirtas/Long/McAllister ......
  - The highest negative tadpole values of explicitly considered model is $-Q_3 = 149$ Crino/Quevedo/Valandro.

Orientifold Calabi-Yau threefold landscape

- toric CY3 hypersurface $(\# <?\mathcal{O}(10^{920}))$ Borisov/Batyrev/Cox/Kreuzer/Skarke/ Demirtas/Long/McAllister ......
  - The highest negative tadpole values of explicitly considered model is $-Q_3 = 149$ Crino/Quevedo/Valandro.
  - We constructed explicitly the toric orientifold CYs with divisor exchange from the $700,000$ toric CYs with $h^{1,1} \leq 6$ and get around 6000 orientifold CYs Altman/Carifio/XG/Nelson JHEP 03 (2022) 087.
    We also make a prediction of orientifold CYs for $h^{1,1} = 7$ by machine learning XG/Zou Phys.Rev.D 105 (2022) 4, 046017.

    The largest negative tadpole is $-Q_3 = 30$ for the concrete SO(8) model and is bounded by $-Q_3 \leq 252$ in Kreuzer-Skarke dataset ($h^{1,1} \leq 491$).

Orientifold Calabi-Yau threefold landscape

- toric CY3 hypersurface ($\# <?\mathcal{O}(10^{920})$) Borisov/Batyrev/Cox/Kreuzer/Skarke/ Demirtas/Long/McAllister ......
    - The highest negative tadpole values of explicitly considered model is $-Q_3 = 149$ Crino/Quevedo/Valandro.
    - We constructed explicitly the toric orientifold CYs with divisor exchange from the $700,000$ toric CYs with $h^{1,1} \leq 6$ and get around 6000 orientifold CYs Altman/Carifio/XG/Nelson JHEP 03 (2022) 087.
      We also make a prediction of orientifold CYs for $h^{1,1} = 7$ by machine learning XG/Zou Phys.Rev.D 105 (2022) 4, 046017.
      The largest negative tadpole is $-Q_3 = 30$ for the concrete SO(8) model and is bounded by $-Q_3 \leq 252$ in Kreuzer-Skarke dataset ($h^{1,1} \leq 491$).
- Complete Intersection Calabi-Yau threefolds (CICY) Hubsch/Candelas/Dale/ Lutaken/Schimmrigk/Green

Orientifold Calabi-Yau threefold landscape

- toric CY3 hypersurface ($\# <?\mathcal{O}(10^{920})$) Borisov/Batyrev/Cox/Kreuzer/Skarke/ Demirtas/Long/McAllister ......
  - The highest negative tadpole values of explicitly considered model is $-Q_3 = 149$ Crino/Quevedo/Valandro.
  - We constructed explicitly the toric orientifold CYs with divisor exchange from the $700,000$ toric CYs with $h^{1,1} \leq 6$ and get around 6000 orientifold CYs Altman/Carifio/XG/Nelson JHEP 03 (2022) 087.
    We also make a prediction of orientifold CYs for $h^{1,1} = 7$ by machine learning XG/Zou Phys.Rev.D 105 (2022) 4, 046017.
    The largest negative tadpole is $-Q_3 = 30$ for the concrete SO(8) model and is bounded by $-Q_3 \leq 252$ in Kreuzer-Skarke dataset ($h^{1,1} \leq 491$).
- Complete Intersection Calabi-Yau threefolds (CICY) Hubsch/Candelas/Dale/ Lutaken/Schimmrigk/Green
  - Based on the favorable Complete Intersection Calabi-Yau (CICY) database ($\# =$ 7890) Anderson/XG/Gray/Lee JHEP 10(2017)007,
    the largest negative tadpole is $-Q_3 = 132.$ Carta/Moritz/Westphal

Orientifold Calabi-Yau threefold landscape

- toric CY3 hypersurface ($\# <? \mathcal{O}(10^{920})$) Borisov/Batyrev/Cox/Kreuzer/Skarke/ Demirtas/Long/McAllister ......
  - The highest negative tadpole values of explicitly considered model is $-Q_3 = 149$ Crino/Quevedo/Valandro.
  - We constructed explicitly the toric orientifold CYs with divisor exchange from the $700,000$ toric CYs with $h^{1,1} \leq 6$ and get around 6000 orientifold CYs Altman/Carifio/XG/Nelson JHEP 03 (2022) 087.
    We also make a prediction of orientifold CYs for $h^{1,1} = 7$ by machine learning XG/Zou Phys.Rev.D 105 (2022) 4, 046017.

    The largest negative tadpole is $-Q_3 = 30$ for the concrete SO(8) model and is bounded by $-Q_3 \leq 252$ in Kreuzer-Skarke dataset ($h^{1,1} \leq 491$).
- Complete Intersection Calabi-Yau threefolds (CICY) Hubsch/Candelas/Dale/ Lutaken/Schimmrigk/Green
  - Based on the favorable Complete Intersection Calabi-Yau (CICY) database ($\# =$ 7890) Anderson/XG/Gray/Lee JHEP 10(2017)007,

    the largest negative tadpole is $-Q_3 = 132.$ Carta/Moritz/Westphal
- Generalized Complete Intersection Calabi-Yau Manifolds (gCICY)
  Anderson/Apruzzi/XG/Gray/Lee Nucl.Phys.B 906(2016)441
  By using ML, we can generate $\# > 4000$ Cui/XG/Wang Phys.Rev.D107(2023)8,086004

Constraint of de-Sitter from Warping correction

- Warping correction is important: the constraints come from demanding that warping corrections in the bulk, associated with the KS throat housing the anti-D3 brane uplift are under control.
  - For KKLT, singular bulk problem is independent from concrete parameters of CYs.
  - For LVS, the parameter control regime is given, but the proper CYs need to be find out if it exist.

Outline

Calabi-Yau 3-folds database

- CICY (# 7890), gCICY ($\# > \mathcal{O}(10^3)$) and toric CY ($\# > \mathcal{O}(10^{10})$).
  Candelas/Dale/Lutken/Schimmrigk, Anderson/XG/Gray/Lee, Anderson/Apruzzi/XG/Gray/Lee, Kreuzer/Skarke, Altman/Gray/He/Jejjala/Nelson

$$X_{\text{CICY}} = \left[\begin{array}{c||ccc} \mathbb{P}^2 & 1 & 1 & 1 \\ \mathbb{P}^4 & 3 & 1 & 1 \end{array} \right], \quad X_{\text{gCICY}} = \left[\begin{array}{c||cc|cc} \mathbb{P}^1 & 1 & 1 & -1 & 1 \\ \mathbb{P}^1 & 1 & 1 & 1 & -1 \\ \mathbb{P}^5 & 3 & 1 & 1 & 1 \end{array} \right]$$

Calabi-Yau 3-folds database

- CICY (# 7890), gCICY ($\# > \mathcal{O}(10^3)$) and toric CY ($\# > \mathcal{O}(10^{10})$).
  Candelas/Dale/Lutken/Schimmrigk, Anderson/XG/Gray/Lee, Anderson/Apruzzi/XG/Gray/Lee, Kreuzer/Skarke, Altman/Gray/He/Jejjala/Nelson

$$X_{\text{CICY}} = \left[\begin{array}{c||ccc} \mathbb{P}^2 & 1 & 1 & 1 \\ \mathbb{P}^4 & 3 & 1 & 1 \end{array} \right], \quad X_{\text{gCICY}} = \left[\begin{array}{c||cc|cc} \mathbb{P}^1 & 1 & 1 & -1 & 1 \\ \mathbb{P}^1 & 1 & 1 & 1 & -1 \\ \mathbb{P}^5 & 3 & 1 & 1 & 1 \end{array} \right]$$

- Orientifold involution

$$\sigma = \begin{cases} \text{Reflection} : \{ x_i \leftrightarrow -x_i, \cdots \} & h^{1,1}_-(X) = 0 \\ \text{Exchange involution} : \{ x_i \leftrightarrow x_j, \cdots \} & h^{1,1}_-(X) \neq 0 \end{cases}$$

Calabi-Yau 3-folds database

- CICY (# 7890), gCICY ($\# > \mathcal{O}(10^3)$) and toric CY ($\# > \mathcal{O}(10^{10})$).
  Candelas/Dale/Lutken/Schimmrigk, Anderson/XG/Gray/Lee, Anderson/Apruzzi/XG/Gray/Lee, Kreuzer/Skarke, Altman/Gray/He/Jejjala/Nelson

$$X_{\text{CICY}} = \left[\begin{array}{c||ccc} \mathbb{P}^2 & 1 & 1 & 1 \\ \mathbb{P}^4 & 3 & 1 & 1 \end{array}\right], \quad X_{\text{gCICY}} = \left[\begin{array}{c||cc|cc} \mathbb{P}^1 & 1 & 1 & -1 & 1 \\ \mathbb{P}^1 & 1 & 1 & 1 & -1 \\ \mathbb{P}^5 & 3 & 1 & 1 & 1 \end{array}\right]$$

- Orientifold involution

$$\sigma = \begin{cases} \text{Reflection} : \{x_i \leftrightarrow -x_i, \cdots\} & h^{1,1}_-(X) = 0 \\ \text{Exchange involution} : \{x_i \leftrightarrow x_j, \cdots\} & h^{1,1}_-(X) \neq 0 \end{cases}$$

  $h^{1,1}_-(X) \neq 0$ is important to solve the chirality issue for global model building (Combine partical physics and moduli stabilization and inflation in a single set-up). Blumenhagen/Moster/Plauschinn, Cicoli/Mayrhofer/Valandro/Quevedo/Krippendorf, Balasubramanian/Berglund/Braun/Garcia-Etxebarria, Grimm/Weigand/Kerstan $\cdots$

  - D-brane at singularity
  - Fluxed Instanton

Searching and Classification of Orientifold CY3s

- Based in the favorable CICY database Anderson/XG/Gray/Lee JHEP10(2017)077, orientifold CICYs has been studied recently. Carta/Moritz/Westphal

Searching and Classification of Orientifold CY3s

- Based in the favorable CICY database Anderson/XG/Gray/Lee JHEP10(2017)077, orientifold CICYs has been studied recently. Carta/Moritz/Westphal
- Favorable Description: When Toric divisor classes on the Calabi-Yau hypersurface X are all descended from ambient space $\mathcal{A}$.

$$h^{1,1}(X) = \dim(H^{1,1}(X)) \cong \dim(\mathrm{Pic}(\mathcal{A})) = h^{1,1}(\mathcal{A})$$

http://www1.phys.vt.edu/cicydata/

The Favorable CICY List, and its Fibrations

Data associated to the paper arXiv:1708.07907

Maximally Favorable CICY List

In arXiv:1708.07907, a favorable configuration has been found for all but 48 CICY three-folds. The remaining CICYs can be described favorably in products of almost del Pezzo surfaces. This website holds the data describing these new descriptions of CICYs. Any use of this data should be acknowledged by referencing the associated publication given above.

The new version of the CICY list, with non-favorable configuration matrices replaced by favorable ones (the "favourable CICY list"), can be found here:

- Text file containing the Favorable CICY list in a Mathematica readable format (3MB)

Hodge data and the second chern class of the manifolds are included. In addition, a flag indicates whether the Kahler cone is the naive one induced from the ambient space. See arXiv:1708.07907 for more details and explanation of format.

Obvious Fibrations

The elliptic fibrations which can be observed directly from the configuration matrices of the favorable CICY list can be found here:

- Text file (12.5 MB)

The data is in the format described in Appendix E of arXiv:1708.07907 and includes elliptic and K3 fibrations as well as nestings of these possibilties. This list only contains 7868 configurations, as the 22 direct product CICYs are excluded. Any use of the data on this website should be acknowledged by referencing the associated publication given above.

Searching and Classification of Orientifold CY3s

- Based in the favorable CICY database Anderson/XG/Gray/Lee JHEP10(2017)077, orientifold CICYs has been studied recently. Carta/Moritz/Westphal
- Favorable Description: When Toric divisor classes on the Calabi-Yau hypersurface X are all descended from ambient space $\mathcal{A}$.

$$h^{1,1}(X) = \dim(H^{1,1}(X)) \cong \dim(\mathrm{Pic}(\mathcal{A})) = h^{1,1}(\mathcal{A})$$

- In toric CY database Altman/Gray/He/Jejjala/Nelson, exchange involution is studied for $h^{1,1} \leq 4$ ($\# \sim \mathcal{O}(10^3)$) XG /Shukla, JHEP11(2013)170 and now for $h^{1,1} \leq 6$ with fully classification of exchange involutions, fix-point locus and free action. Altman/Carifio/ XG /Nelson, JHEP03(2022)087

Searching and Classification of Orientifold CY3s

- Based in the favorable CICY database Anderson/XG/Gray/Lee JHEP10(2017)077, orientifold CICYs has been studied recently. Carta/Moritz/Westphal
- Favorable Description: When Toric divisor classes on the Calabi-Yau hypersurface X are all descended from ambient space $\mathcal{A}$.

$$h^{1,1}(X) = \dim(H^{1,1}(X)) \cong \dim(\mathrm{Pic}(\mathcal{A})) = h^{1,1}(\mathcal{A})$$

- In toric CY database Altman/Gray/He/Jejjala/Nelson, exchange involution is studied for $h^{1,1} \leq 4$ ($\# \sim \mathcal{O}(10^3)$) XG /Shukla, JHEP11(2013)170 and now for $h^{1,1} \leq 6$ with fully classification of exchange involutions, fix-point locus and free action. Altman/Carifio/ XG /Nelson, JHEP03(2022)087
- Among total 646903 CYs with $h^{1,1}(X) \leq 6$, only 5% of them admits a proper divisor exchange orientifold.
- Most of oreintifold CYs admitting an $O3/O7$ system, 60% of them admitting a naive orientifold Type IIB string vacua.

Searching and Classification of Orientifold CY3s

- Based in the favorable CICY database Anderson/XG/Gray/Lee JHEP10(2017)077, orientifold CICYs has been studied recently. Carta/Moritz/Westphal
- Favorable Description: When Toric divisor classes on the Calabi-Yau hypersurface X are all descended from ambient space $\mathcal{A}$.

$$h^{1,1}(X) = \dim(H^{1,1}(X)) \cong \dim(\mathrm{Pic}(\mathcal{A})) = h^{1,1}(\mathcal{A})$$

- In toric CY database Altman/Gray/He/Jejjala/Nelson, exchange involution is studied for $h^{1,1} \leq 4$ ($\# \sim \mathcal{O}(10^3)$) XG /Shukla, JHEP11(2013)170 and now for $h^{1,1} \leq 6$ with fully classification of exchange involutions, fix-point locus and free action. Altman/Carifio/ XG /Nelson, JHEP03(2022)087
- Among total 646903 CYs with $h^{1,1}(X) \leq 6$, only 5% of them admits a proper divisor exchange orientifold.
- Most of oreintifold CYs admitting an $O3/O7$ system, 60% of them admitting a naive orientifold Type IIB string vacua.
- Suitable for Machine Learning to extend our result to higher $h^{1,1}$ to search and classify orientifold CYs. XG /Zhou Phys.Rev.D.105(2022)4,046017
- Based on our works, some new progress is under going. Crino/Quevedo/ Schachner/Valandro, Hongfei Gao/XG

Current status of constructing orientifold CY

- We identify the topology of each divisors and determine the involutions which are globally consistent across all disjoint phases of the Kähler cone for each unique CY.
- Identify free action of involution and all possible fixed loci under non-trivial actions, thereby determining the type and location of O-planes.

Current status of constructing orientifold CY

- We identify the topology of each divisors and determine the involutions which are globally consistent across all disjoint phases of the Kähler cone for each unique CY.
- Identify free action of involution and all possible fixed loci under non-trivial actions, thereby determining the type and location of O-planes.
- Classify the naive orientifold string vacua by considering the D3 tadpole cancelation locally.
- Determine the Hodge number splitting under these involutions.

Current status of constructing orientifold CY

- We identify the topology of each divisors and determine the involutions which are globally consistent across all disjoint phases of the Kähler cone for each unique CY.
- Identify free action of involution and all possible fixed loci under non-trivial actions, thereby determining the type and location of O-planes.
- Classify the naive orientifold string vacua by considering the D3 tadpole cancelation locally.
- Determine the Hodge number splitting under these involutions.
- The ML method gives a very high precision (99.96%) for identifying the polytopes which can result in an orientifold CY. This indicate the orientifold symmetry may encoded in the polytope structure itself.
- The ML method predict the polytopes which can result in an orientifold CY for higher h^{11}.

Proper Involution σ

Proper Involutions $\sigma : x_i \leftrightarrow x_j \quad \Longrightarrow \quad \sigma^* : D_i \leftrightarrow D_j$.

- In favorable case, restricts strightforward to the Calabi-Yau hypersurface.
- $D_\pm = D_i \pm D_j \in H^{1,1}_\pm(X/\sigma^*)$
- Non-Trivial Identity Divisor: $H^\bullet(D_i) \cong H^\bullet(D_j)$ with different wights $\mathcal{O}(D)$.
  - Completely Rigid Divisors:
    $h^\bullet(D) = \{h^{0,0}(D), h^{0,1}(D), h^{0,2}(D), h^{1,1}(D)\} = \{1, 0, 0, h^{1,1}(D)\}$.
    Wilson Divisors: $h^\bullet(W) = \{1, h^{1,0}, 0, h^{1,1}\}$. $h^{1,0}_+ = 1$ characterize the zero modes of poly-instanton, which can't be lifted by background fluxes.
    Deformation divisors such as $K3$.
- Symmetry of Stanley-Reisner Ideal $\mathcal{I}_{SR}(\mathcal{A})$: To ensure the involution to be an automorphism of $\mathcal{A}$, leaving invariant the exceptional divisors from resolved singularities.
- Symmetry of the linear ideal $\mathcal{I}_{lin}(\mathcal{A})$: To ensures the defining polynomial of CY remains homogeneous under involution.

$$A^\bullet(\mathcal{A}) \cong \frac{\mathbb{Z}(D_1, \cdots, D_k)}{\mathcal{I}_{lin}(\mathcal{A}) + \mathcal{I}_{SR}(\mathcal{A})} .$$

- Triple intersection tensor defined in Chow ring should be invariant under involution σ.

Example: $h^{1,1}(X) = 4, h^{2,1}(X) = 64.$

x_1	x_2	x_3	x_4	x_5	x_6	x_7	x_8
0	0	0	1	0	1	0	0
0	0	1	0	0	0	1	0
0	1	0	0	1	0	0	1
1	0	0	1	0	0	1	1

- $\mathcal{I}_{SR} = \langle x_1 x_8,\ x_3 x_7,\ x_4 x_6,\ x_1 x_4 x_7,\ x_2 x_3 x_5,\ x_2 x_5 x_6,\ x_2 x_5 x_8 \rangle$

The linear ideal, which fixes toric divisor redundancies, is given by

$$\mathcal{I}_{lin} = \begin{array}{ccccccccccccccccc} \langle & -D_1 & - & D_2 & - & D_3 & - & D_4 & + & 0 & + & D_6 & + & D_7 & + & D_8, & \\ + & 0 & + & 0 & + & D_3 & + & D_4 & + & 0 & - & D_6 & - & D_7 & & 0, & \\ - & D_1 & & 0 & - & D_3 & - & D_4 & - & D_5 & + & D_6 & + & D_7 & + & D_8, & \\ + & 0 & + & 0 & + & 0 & + & D_4 & + & D_5 & - & D_6 & + & 0 & - & D_8 & \rangle, \end{array}$$

and a basis in $H^{1,1}(X;\mathbb{Z})$ given by $J_1 = D_1,\ J_2 = D_2,\ J_3 = D_3,\ J_4 = D_6$.

- Determine the topology of divisor

$$h^\bullet(D_1) = \{1,0,0,9\}, \quad h^\bullet(D_2) = h^\bullet(D_4) = h^\bullet(D_5) = h^\bullet(D_7) = \{1,0,1,21\}$$
$$h^\bullet(D_3) = h^\bullet(D_6) = \{1,0,0,12\}, \quad h^\bullet(D_8) = \{1,0,2,30\}$$

- Exist only one proper involution: $\sigma : x_3 \leftrightarrow x_6,\ \ x_4 \leftrightarrow x_7$

Since $\sigma^*\Omega_3 = -\Omega_3$, one would expect $O3/O7$-system.

Hodge Number Splitting

- Orientifold plane

$$F_1 = \{x_3 x_4 - x_6 x_7 = 0\}, \;\; F_2 = \{x_1 = x_2 = x_5 = 0\}$$

we can determine F_1 is an O7 plane, while F_2 is an O3 plane locus.

- String vacua (local model)

$$N_{D3} + \frac{N_{\text{flux}}}{2} + N_{\text{gauge}} = \frac{N_{O3}}{4} + \frac{\chi(D_{O7})}{4} = \frac{1+39}{4} = 10\,.$$

"naive orientifold type IIB string vacua".

- Hodge number splitting

$$h^{1,1}_{+}(X/\sigma^*) = 3, \qquad h^{1,1}_{-}(X/\sigma^*) = 1$$

Orientifold CY Database I

$\mathbf{h^{1,1}(X)}$	**1**	**2**	**3**	**4**	**5**	**6**	**Total**
# of Favorable Polytopes	5	36	243	1185	4897	16608	22974
# of Favorable Triangulations	5	48	525	5330	56714	584281	646903
# of Favorable Geometries	5	39	305	2000	13494	84525	100368
% of Favorable Triangulations Scanned	80	100	99.8	99.66	99.41	99.01	99.01

Table 1: The favorable polytopes, triangulations, geometries for $h^{1,1}(X) \leq 6$.

Orientifold CY Database II

$h^{1,1}(X)$	1	2	3	4	5	6	Total
Triangulation-wise proper NID exchange involutions							
# of Polytopes contains Involutions	0	1	25	166	712	2172	3076
# of Geometries contains Involutions	0	1	26	273	1559	6590	8449
# of Triangulations contains Involutions	0	1	31	405	3372	21566	25375
# of Involutions	0	6	51	516	4085	23805	28463
Geometry-wise proper NID exchange involutions							
# of Polytope contains Involutions	0	1	16	96	330	958	1401
# of Geometries contains Involutions	0	1	17	183	911	3370	4482
# of Involutions	0	6	28	259	1219	4148	5660
% of Polytope contains Involutions	0	2.78	6.58	8.10	6.74	5.77	6.10
% of Geometries contains Involutions	0	2.56	5.57	9.15	6.75	3.99	4.47

Table 2: Statistic counting on the triangulation/geometry-wide Non-trivial Identical Divisors exchange involutions in favorable polytopes, triangulations and geometries.

Orientifold CY Database III

Number of pairs of Non-trivial Identical Divisors (NID) under involutions							
$h^{1,1}(X)$	**1**	**2**	**3**	**4**	**5**	**6**	**Total**
Triangulation-wise proper Involutions							
# of Involutions	0	6	51	516	4085	23805	28463
del Pezzo surface dP_n, $n \le 8$	0	0	12	238	2233	14507	17090
Rigid surface dP_n, $n > 8$	0	0	14	512	5659	32481	38666
(exact-)Wilson surface	0 (0)	0 (0)	5 (0)	40 (5)	177 (80)	744 (411)	966 (496)
K3 surface	0	0	65	300	619	1976	2960
SD1 surface	0	0	9	47	418	2190	2664
SD2 surface	0	18	8	33	109	459	627
del Pezzo and K3	0	0	0	9	98	572	679
del Pezzo and (Exact-)Wilson	0 (0)	0 (0)	1 (0)	28 (0)	95 (9)	667 (286)	791 (295)
K3 and (Exact-)Wilson	0 (0)	0 (0)	8 (0)	12 (4)	43 (7)	101 (9)	156 (20)
del Pezzo, K3 and (Exact-)Wilson	0 (0)	0 (0)	0 (0)	0 (0)	28 (0)	87 (2)	115 (2)
Geometry-wise proper Involutions							
# of Involutions	0	6	28	259	1219	4148	5660
del Pezzo surface dP_n, $n \le 8$	0	0	8	107	634	2660	3409
Rigid surface dP_n, $n > 8$	0	0	8	259	1973	6198	8438
(Exact-)Wilson surface	0 (0)	0 (0)	5 (0)	28 (2)	48 (4)	136 (75)	217 (81)
K3 surface	0	0	28	215	219	527	989
SD1 surface	0	0	8	23	102	216	349
SD2 surface	0	18	6	18	39	84	165
del Pezzo and K3	0	0	0	0	26	156	182
del Pezzo and (Exact-)Wilson	0 (0)	0 (0)	1 (0)	19 (0)	40 (1)	109 (40)	169 (41)
K3 and (Exact-)Wilson	0 (0)	0 (0)	8 (0)	12 (4)	13 (4)	23 (3)	56 (11)
del Pezzo, K3 and (Exact-)Wilson	0 (0)	0 (0)	0 (0)	0 (0)	4 (0)	16 (2)	20 (2)

Orientifold CY Database IV

Classification of O-plane fixed point locus							
$h^{1,1}(X)$	**1**	**2**	**3**	**4**	**5**	**6**	**Total**
Triangulation-wise proper Involutions							
# of Involutions	0	6	51	516	4085	23772	28430
O3	0	0	9	253	2640	18193	21083
O5	0	6	20	157	1006	3279	4468
O7	0	0	31	328	3005	20137	23501
O3 and O7	0	0	9	222	2566	17826	20623
Free Action	0	0	0	0	0	1	1
Geometry-wise proper Involutions							
# of Involutions	0	6	28	259	1219	4148	5660
O3	0	0	4	82	557	2611	3254
O5	0	6	16	106	488	929	1545
O7	0	0	12	124	691	3082	3909
O3 and O7	0	0	4	53	523	2475	3055
Free Action	0	0	0	0	0	1	1

Table 4: Classification of O-plane fixed point locus and free actions under the triangulation/geometry-wise proper involutions.

Orientifold CY Database V

Naive Orientifold Type IIB String Vacua with $O3/O7$-system							
$\mathbf{h^{1,1}(X)}$	**1**	**2**	**3**	**4**	**5**	**6**	**Total**
Triangulation-wise proper Involutions							
# of Involutions	0	6	51	516	4085	23772	28430
Contains O3 & O7	0	0	9	206	2346	15234	17795
Contains Only O3	0	0	0	31	74	355	460
Contains Only O7	0	0	22	102	386	1950	2460
Total String Vacua	0	0	31	339	2806	17539	20715
Geometry-wise proper Involutions							
# of Involutions	0	6	28	259	1219	4148	5660
Contains O3 & O7	0	0	4	48	455	1874	2381
Contains Only O3	0	0	0	29	34	136	199
Contains Only O7	0	0	8	68	149	529	754
Total String Vacua	0	0	12	145	638	2539	3334

Table 5: Classification of naive orientifold Type IIB string vacua under the triangulation/geometry-wise proper involutions.

Orientifold CY Database VI

Hodge number splitting								
$h^{1,1}(X)$		1	2	3	4	5	6	Total
Triangulation-wide proper Involutions								
# of Involutions		0	6	51	516	4085	23805	28463
# of $h^{1,1}_-$	1	–	6	51	477	3682	20985	25201
	2	–	–	0	39	483	2618	3140
	3	–	–	–	0	0	202	202
	4	–	–	–	–	0	0	0
	5	–	–	–	–	–	0	0
Geometry-wide proper Involutions								
# of Involutions		0	6	28	259	1219	4148	5660
# of $h^{1,1}_-$	1	–	6	28	277	1048	3413	4772
	2	–	–	0	32	171	661	864
	3	–	–	–	0	0	74	74
	4	–	–	–	–	0	0	0
	5	–	–	–	–	–	0	0

Table 6: Classification of $h^{1,1}(X/\sigma^*)$ splitting under the triangulation/geometry-wise proper involutions.

Database

http://www.rossealtman.com/toriccy. Altman/Carifio/ XG /Nelson, JHEP03(2022)087

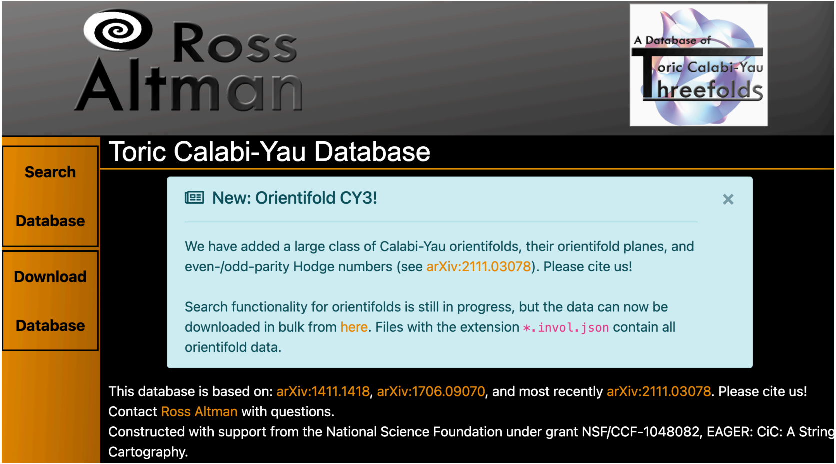

Why Machine Learning?

XG /Zhou Phys.Rev.D.105(2022)4,046017

- Whether ML can pick out the orientifold property of a CYs.
- It was conjectured that the orientifold symmetry (at least the involution symmetry) on the CYs is already encoded in the polytope structure.
- Hard for higher $h^{1,1}$. Three difficulties.
- Rare Signal (around 5% for $h^{1,1} \leq 6$). It would be great even if we just train our machine to narrow down the candidate pool and increase the successful rate by one order.
- Training data: 22960 polytopes, among them 1402 can result in an exchange orientifold CYs and 996 can end up with a naive string vacua.
- Enlarge the data by 120 permutations: 2755200 training data.

	Unresolved	Resolved
Orientifold	99.906%	99.907%
Naive Type IIB string vacua	99.802%	99.897%

Table 1: Test results for $h^{1,1} \leq 6$.

Accuracy of classifier

Accuracy for unresolved data: 99.906% for orientifold & 99.802% for vacua.

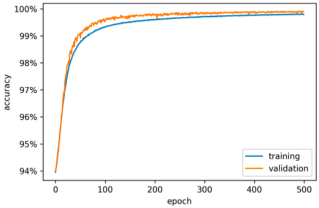

(a) Orientifold

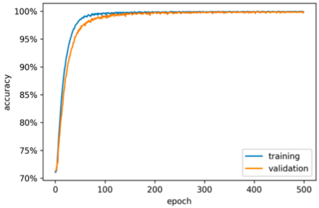

(b) Geometry-wise string vacua

Accuracy for resolved data: 99.907% for orientifold & 99.897% for vacua.

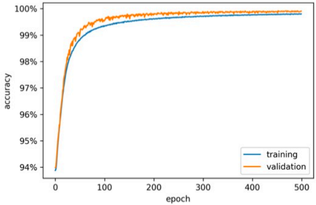

(a) Orientifold

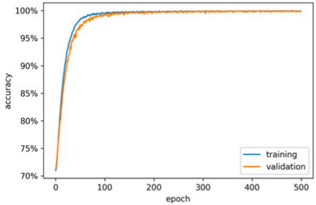

(b) Geometry-wise string vacua

Prediction for $h^{1,1}(X) = 7$

- Initial data: 50376 unresolved polytopes $\ll$ trained data (2755200)
- The trained model with parameters fixed.
- After classifier, among the polytopes with $h^{1,1} = 7$, 2086 of them may end up with orientifold CYs

$\mathbf{h^{1,1}(X)}$	**1**	**2**	**3**	**4**	**5**	**6**	**7**
# of Trianed Polytopes	5	36	243	1185	4897	16608	50376
# of "orientifold" Polytopes	0	1	16	96	330	958	2086
% of "orientifold" Polytopes	0	2.78	6.58	8.10	6.74	5.77	4.14

Table 2: Statistic counting on the polytopes which can result in orientifold Calabi-Yau. The result for $h^{1,1} \leq 6$ comes from [1] while for $h^{1,1} = 7$ comes from our trained neural network.

Working in Progress Hongfei Gao/XG

- Extend to higher $h^{1,1}(X)$ by using random triangulation method inspired by graph theory Demirtas/Long/McAllister/Stillman
- Supervised training by generating enough initial orientifold CYs (we only need 30% of the data to train to get a high accuracy for $h^{1,1} \leq 6$). Use a subset of the database to learn something more complicated.

Ratio of Training Data	30%	20%	10%
Training Accuracy	99.70%	99.64%	99.22%
Validation Accuracy	99.75%	99.16%	91.90%
Test Accuracy	99.76%	99.14%	91.64%

- Including all exchange involution and triple reflection involution for all CY with $h^{1,1}(X) \leq 7$

Example of $h^{1,1} = 6, h^{2,1} = 42$

x_1	x_2	x_3	x_4	x_5	x_6	x_7	x_8	x_9	x_{10}
1	0	0	0	0	0	1	1	0	1
2	2	1	1	0	0	2	0	2	2
1	1	1	1	0	0	0	0	0	0
3	1	1	1	2	0	4	0	0	0
0	0	0	0	0	1	0	0	0	1
0	0	0	0	0	0	1	0	1	0

- $\mathcal{I}_{SR} = \langle x_1x_2,\ x_1x_5,\ x_1x_8,\ x_2x_5,\ x_2x_9,\ x_2x_{10},\ x_3x_4,\ x_5x_6,\ x_6x_7x_8,\ x_6x_{10},\ x_7x_9,\ x_8x_{10}\rangle$
- $h^\bullet(D_i) = \{1, 0, 1, 20\}$ for i = 1, 3, 4, 7 $h^\bullet(D_j) = \{1, 1, 0, 6\}$ for j = 8, 9
- in total $9 + \frac{9*8}{2} + \frac{9*8*7}{6} = 129$ reflections.
- $\sigma_1 : x_1 \leftrightarrow -x_1 :\ [[x_1], [x_2], [x_6, x_8, x_9]], \# O3 : 4$
- $\sigma_2 : x_{1,3} \leftrightarrow -x_{1,3} :\ [[x_1, x_3], [x_1, x_4], [x_2, x_3], [x_2, x_4]]$
- $\sigma_3 : x_{1,2,3} \leftrightarrow -x_{1,2,3} :\ [[x_3], [x_4]]$
- no proper divisor exchange involution

gCICY Anderson/Apruzzi/XG/Gray/Lee Nucl.Phys.B 906(2016)441

$$X = \left[\begin{array}{c||cc|cc} \mathbb{P}^1 & 1 & 1 & -1 & 1 \\ \mathbb{P}^1 & 1 & 1 & 1 & -1 \\ \mathbb{P}^5 & 3 & 1 & 1 & 1 \end{array} \right] \quad \mathcal{M} = \left[\begin{array}{c||cc} \mathbb{P}^1 & 1 & 1 \\ \mathbb{P}^1 & 1 & 1 \\ \mathbb{P}^5 & 3 & 1 \end{array} \right]$$

- $X \overset{②}{\hookrightarrow} \mathcal{M} \overset{①}{\hookrightarrow} \mathcal{A}$ ②: $h^0(\mathcal{M}, \mathcal{O}_{\mathcal{M}}(1,-1,1)) = h^0(\mathcal{M}, \mathcal{O}_{\mathcal{M}}(-1,1,1)) = 1$
  $\Rightarrow$ Polynomial description in $\mathcal{M}$ " $\equiv$ " Rational description by $\mathbf{x} \in \mathcal{A}$
  ①, ② are algebraic complete intersection.
- Rational description $\Rightarrow$ "non-polynomail " deformations

Candelas, De La Ossa, Font, Katz, Morrison, Green, Hubsch, Mavlyutov,...

gCICY

Anderson/Apruzzi/XG/Gray/Lee Nucl.Phys.B 906(2016)441

$$X = \left[\begin{array}{c||cc|cc} \mathbb{P}^1 & 1 & 1 & -1 & 1 \\ \mathbb{P}^1 & 1 & 1 & 1 & -1 \\ \mathbb{P}^5 & 3 & 1 & 1 & 1 \end{array}\right] \quad \mathcal{M} = \left[\begin{array}{c||cc} \mathbb{P}^1 & 1 & 1 \\ \mathbb{P}^1 & 1 & 1 \\ \mathbb{P}^5 & 3 & 1 \end{array}\right]$$

- $X \overset{②}{\hookrightarrow} \mathcal{M} \overset{①}{\hookrightarrow} \mathcal{A}$ ②: $h^0(\mathcal{M}, \mathcal{O}_{\mathcal{M}}(1,-1,1)) = h^0(\mathcal{M}, \mathcal{O}_{\mathcal{M}}(-1,1,1)) = 1$
  $\Rightarrow$ Polynomial description in $\mathcal{M}$ " $\equiv$ " Rational description by $\mathbf{x} \in \mathcal{A}$
  ①, ② are algebraic complete intersection.
- Rational description $\Rightarrow$ "non-polynomail " deformations
  Candelas, De La Ossa, Font, Katz, Morrison, Green, Hubsch, Mavlyutov,...
- The effective cone of $\mathcal{M}$ is larger than the one in $\mathcal{A}$

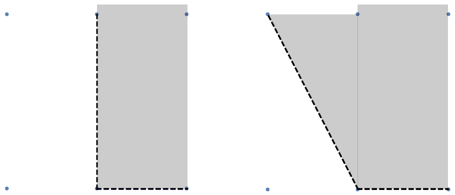

New Hodge Data

$(h^{1,1}(X), h^{1,2}(X))$	X
$(1,91)$	$\left[\begin{array}{c\|\|cc\|c} \mathbb{P}^2 & 1 & 1 & 1 \\ \mathbb{P}^2 & 0 & 3 & 0 \\ \mathbb{P}^1 & 0 & 0 & 2 \\ \mathbb{P}^1 & 1 & 2 & -1 \end{array}\right]$
$(1,109)$	$\left[\begin{array}{c\|\|cc\|c} \mathbb{P}^2 & 1 & 0 & 2 \\ \mathbb{P}^2 & 0 & 3 & 0 \\ \mathbb{P}^1 & 0 & 1 & 1 \\ \mathbb{P}^1 & 1 & 3 & -2 \end{array}\right]$
$(2,98)$	$\left[\begin{array}{c\|\|cc\|c} \mathbb{P}^2 & 1 & 0 & 2 \\ \mathbb{P}^1 & 0 & 2 & 0 \\ \mathbb{P}^1 & 0 & 1 & 1 \\ \mathbb{P}^1 & 0 & 2 & 0 \\ \mathbb{P}^1 & 1 & 3 & -2 \end{array}\right]$
$(6,18)$	$\left[\begin{array}{c\|\|cc\|c} \mathbb{P}^2 & 0 & 1 & 2 \\ \mathbb{P}^1 & 0 & 1 & 1 \\ \mathbb{P}^1 & 1 & 0 & 1 \\ \mathbb{P}^1 & 1 & 0 & 1 \\ \mathbb{P}^1 & 1 & 3 & -2 \end{array}\right], \left[\begin{array}{c\|\|cc\|c} \mathbb{P}^2 & 0 & 1 & 2 \\ \mathbb{P}^1 & 0 & 3 & -1 \\ \mathbb{P}^1 & 1 & 1 & 0 \\ \mathbb{P}^1 & 1 & 0 & 1 \\ \mathbb{P}^1 & 1 & 0 & 1 \end{array}\right], \left[\begin{array}{c\|\|cc\|c} \mathbb{P}^2 & 0 & 1 & 2 \\ \mathbb{P}^1 & 0 & 0 & 2 \\ \mathbb{P}^1 & 1 & 1 & 0 \\ \mathbb{P}^1 & 1 & 3 & -2 \\ \mathbb{P}^1 & 1 & 0 & 1 \end{array}\right]$
$(10,19)$	$\left[\begin{array}{c\|\|cc\|c} \mathbb{P}^2 & 0 & 0 & 3 \\ \mathbb{P}^2 & 1 & 1 & 1 \\ \mathbb{P}^1 & 0 & 1 & 1 \\ \mathbb{P}^1 & 1 & 3 & -2 \end{array}\right], \left[\begin{array}{c\|\|cc\|c} \mathbb{P}^2 & 0 & 0 & 3 \\ \mathbb{P}^2 & 1 & 1 & 1 \\ \mathbb{P}^1 & 1 & 0 & 1 \\ \mathbb{P}^1 & 1 & 5 & -4 \end{array}\right], \left[\begin{array}{c\|\|cc\|c} \mathbb{P}^2 & 0 & 0 & 3 \\ \mathbb{P}^2 & 1 & 1 & 1 \\ \mathbb{P}^1 & 1 & 0 & 1 \\ \mathbb{P}^1 & 2 & 3 & -3 \end{array}\right], \left[\begin{array}{c\|\|cc\|c} \mathbb{P}^2 & 0 & 0 & 3 \\ \mathbb{P}^2 & 2 & 2 & -1 \\ \mathbb{P}^1 & 0 & 1 & 1 \\ \mathbb{P}^1 & 1 & 0 & 1 \end{array}\right]$
$(9,13)$	$\left[\begin{array}{c\|\|cc\|c} \mathbb{P}^3 & 2 & 0 & 2 \\ \mathbb{P}^1 & 0 & 1 & 1 \\ \mathbb{P}^1 & 0 & 1 & 1 \\ \mathbb{P}^1 & 1 & 3 & -2 \end{array}\right], \left[\begin{array}{c\|\|cc\|c} \mathbb{P}^3 & 2 & 0 & 2 \\ \mathbb{P}^1 & 0 & 3 & -1 \\ \mathbb{P}^1 & 0 & 1 & 1 \\ \mathbb{P}^1 & 1 & 1 & 0 \end{array}\right]$
$(9,15)$	$\left[\begin{array}{c\|\|cc\|c} \mathbb{P}^3 & 1 & 0 & 3 \\ \mathbb{P}^1 & 0 & 1 & 1 \\ \mathbb{P}^1 & 1 & 1 & 0 \\ \mathbb{P}^1 & 1 & 3 & -2 \end{array}\right]$
$(10,14)$	$\left[\begin{array}{c\|\|cc\|c} \mathbb{P}^2 & 1 & 0 & 2 \\ \mathbb{P}^1 & 0 & 1 & 1 \\ \mathbb{P}^1 & 0 & 1 & 1 \\ \mathbb{P}^1 & 1 & 3 & -2 \\ \mathbb{P}^1 & 1 & 0 & 1 \end{array}\right], \left[\begin{array}{c\|\|cc\|c} \mathbb{P}^2 & 1 & 0 & 2 \\ \mathbb{P}^1 & 0 & 3 & -1 \\ \mathbb{P}^1 & 0 & 1 & 1 \\ \mathbb{P}^1 & 1 & 1 & 0 \\ \mathbb{P}^1 & 1 & 0 & 1 \end{array}\right], \left[\begin{array}{c\|\|cc\|c} \mathbb{P}^2 & 1 & 0 & 2 \\ \mathbb{P}^1 & 0 & 0 & 2 \\ \mathbb{P}^1 & 0 & 1 & 1 \\ \mathbb{P}^1 & 1 & 1 & 0 \\ \mathbb{P}^1 & 1 & 3 & -2 \end{array}\right]$

Table 13: The Hodge pairs and configuration matrices of novel codimension (2,1) examples. These new Hodge pairs do not appear in the regular CICY list [2], Kreuzer-Skarke list [29] or elsewhere in the known literature [58].

Machine Learning to predict more gCICY

Cui/XG/Wang Phys.Rev.D 107 (2023) 8, 086004

Embedding projective spaces	# of classes of generalized configuration matrices	# of spaces found in previous scan [6]	# of spaces found in our scan
$\mathbb{P}^5 \times \mathbb{P}^1$	168	28	67
$\mathbb{P}^4 \times \mathbb{P}^2$	210	6	9
$\mathbb{P}^4 \times \mathbb{P}^1 \times \mathbb{P}^1$	1,197	229	369
$\mathbb{P}^3 \times \mathbb{P}^2 \times \mathbb{P}^1$	1,800	263	341
$\mathbb{P}^2 \times \mathbb{P}^2 \times \mathbb{P}^2$	550	12	12
$\mathbb{P}^3 \times \mathbb{P}^1 \times \mathbb{P}^1 \times \mathbb{P}^1$	4,410	545	860
$\mathbb{P}^2 \times \mathbb{P}^2 \times \mathbb{P}^1 \times \mathbb{P}^1$	5,235	520	683
$\mathbb{P}^2 \times \mathbb{P}^1 \times \mathbb{P}^1 \times \mathbb{P}^1 \times \mathbb{P}^1$	12,180	770	1098
$\mathbb{P}^1 \times \mathbb{P}^1 \times \mathbb{P}^1 \times \mathbb{P}^1 \times \mathbb{P}^1 \times \mathbb{P}^1$	8,442	360	523
Total	34,192	2,733	3,962

TABLE I. The distribution of codimension $(2, 1)$ gCICYs founded in products of projective spaces.

Outline

Summary and outlook

- Various corrections in orientifold Type IIB string JHEP09(2022)091.
- The parameter constraint in realizing de-Sitter space in string theory
  - Warping correction: Singular Bulk problem in KKLT Fortsch.Phys.68(2020)200089 and Parameter Tadpole Constraint in LVS JHEP07(2022)056
  - Potential danger in fiber inflation by log enhancement of α'^4 correction and the new correction beyond BHP conjecture working
  - New uplift mechanism to relax the constraint
  - Searching new topology of orientifold CY or searching new CY to make the constraint less stringent working
- Generate more complete orientifold CY with all exchange involutions and sufficient reflections JHEP03(2022)087, working
- Using ML to predict string vacua in a large-scale CY compactifications Phys.Rev.D.105(2022)4,046017, Phys.Rev.D.107(2023)8, 086004, working

Thanks for your attention!